Computational Studies on the Platinum(II)-Catalyzed Cycloisomerization of 1,6-Dienes into Bicyclopropanes: A Mechanistic Quandary Evaluated by DFT

ARTICLE *in* ORGANOMETALLICS · APRIL 2009

Impact Factor: 4.13 · DOI: 10.1021/om800760x · Source: PubMed

4 AUTHORS, INCLUDING:

Jason P Holland
Harvard Medical School
66 PUBLICATIONS **1,483** CITATIONS
SEE PROFILE

Jennifer C Green
University of Oxford
393 PUBLICATIONS **8,765** CITATIONS
SEE PROFILE

ORGANOMETALLICS

Article

Computational Studies on the Platinum(II)-Catalyzed Cycloisomerization of 1,6-Dienes into Bicyclopropanes: A Mechanistic Quandary Evaluated by DFT

Franziska Bell, Jason Holland, Jennifer C. Green, and Michel R. Gagne#

Organometallics, **2009**, 28 (7), 2038-2045• DOI: 10.1021/om800760x • Publication Date (Web): 16 March 2009

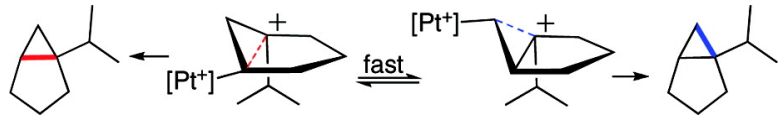

More About This Article

Additional resources and features associated with this article are available within the HTML version:

- Supporting Information
- Access to high resolution figures
- Links to articles and content related to this article
- Copyright permission to reproduce figures and/or text from this article

View the Full Text HTML

Computational Studies on the Platinum(II)-Catalyzed Cycloisomerization of 1,6-Dienes into Bicyclopropanes: A Mechanistic Quandary Evaluated by DFT

Franziska Bell,[†] Jason Holland,[†] Jennifer C. Green,*[,†] and Michel R. Gagné[‡]

The Inorganic Chemistry Laboratory, South Parks Road, Oxford OX1 3QR, United Kingdom, and Department of Chemistry, University of North Carolina at Chapel Hill, Chapel Hill, North Carolina 27599-3290

Received August 6, 2008

The mechanism of the (bis(phosphanylethyl)phosphane)Pt^{2+}-catalyzed cycloisomerization reaction of 7-methylocta-1,6-diene to form 1-isopropylbicyclo[3.1.0]hexane was studied using computational methods. The cyclopropanation step was found to be the turnover-limiting step. The overall reaction proceeds via both a 5-exo and a 6-endo route. W conformations were shown to facilitate cyclopropanation, but do not have any influence on the rate of the 1,2-hydride shifts.

Introduction

The conversion of squalene to hopene by squalene−hopene cyclase (SHC)[1] represents one of the most impressive examples of a cycloisomerization reaction (eq 1).[2] It also highlights the general theme of utilizing polyunsaturation to drive the synthesis of complex multicyclic products in terpene biosynthesis.[3] The key transformation used in the construction of the terpenoids is the cation-olefin reaction, which, because of its ability to regenerate the cationic reactive intermediate, is perfectly suited to cascade polycyclization processes.[4] In the biological context, the initiators of these reactions are typically Brønsted in nature, but metals can also be involved (e.g., Mg^{2+} for pyrophosphate ionization). Initiation and propagation is tightly controlled by the appropriate cyclase enzyme, with preorganization, cation-π, H-bonding, etc., providing the stereo-, regio-, and chemoselectivity in these reactions.

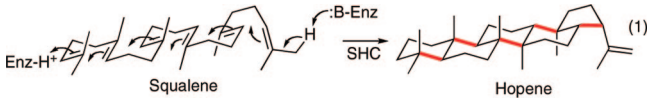

(1)

Transition metal-catalyzed cycloisomerization reactions are some of the most efficient methods for constructing polycyclic products[5] and, like the enzymatic cases, similarly utilize unsaturation to drive the production of polycyclic isomers. Judicious choice of metal catalyst (e.g., Ru,[5] vs Pt[6] vs Au[7]) enables different isomerization pathways to be exploited and unique products to be obtained. One unusual cycloisomerization pathway is the conversion of 1,6- and 1,7-dienes into bicyclopropane products[8] by electrophilic phosphine-ligated Pt(II) dications (e.g., eq 2).[9,10] Like the enzymatic reactions, these processes are thought to proceed via ionic intermediates, though many of the mechanistic details underpinning the transformation are missing.

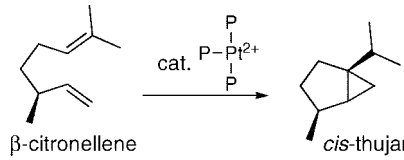

(2)

The illustrated cycloisomerization of β-citronellene to *cis*-thujane typifies a reaction that has a number of similarities to the biosynthesis of the thujane monoterpenes (Scheme 1).[11] Starting from geranyl pyrophosphate, the pathways to the natural products are initiated by the generation of an allyl cation, which undergoes a cation-olefin cyclization to the terpinyl cation **A**,

* Corresponding author. E-mail: jennifer.green@chem.ox.ac.uk.
[†] The Inorganic Chemistry Laboratory.
[‡] University of North Carolina at Chapel Hill.

(1) (a) Wendt, K. U. *Angew. Chem., Int. Ed.* **2005**, *44*, 3966–3971. (b) Reinert, D. J.; Balliano, G.; Schultz, G. E. *Chem. Biol.* **2004**, *11*, 121–126. (c) Hoshimo, T.; Sato, T. *Chem. Commun.* **2002**, 291–301. (d) Wendt, K. U.; Poralla, K.; Schultz, G. E. *Science* **1997**, *277*, 1811–1815.

(2) For an entry into metal-catalyzed cycloisomerization reactions, see: (a) Michelet, V.; Toullec, P. Y.; Genet, J.-P. *Angew. Chem., Int. Ed.* **2008**, *47*, 4268–4315. (b) Diver, S. T.; Giessert, A. J. *Chem. Rev.* **2004**, *104*, 1317–1382. (c) Echavarren, A. M.; Nevado, C. *Chem. Soc. Rev.* **2004**, *33*, 431–436. (d) Méndez, M.; Mamane, V.; Fürstner, A. *Chemtracts* **2003**, *16*, 397–425. (e) Ojima, I.; Tzamarioudaki, M.; Li, Z.; Donovan, R. J. *Chem. Rev.* **1996**, *96*, 635–662.

(3) For a mechanistic discussion of metal-catalyzed cycloisomerization reactions, see: Lloyd-Jones, G. C. *Org. Biomol. Chem.* **2003**, *1*, 215–236. (a) Christianson, D. W. *Chem. Rev.* **2006**, *106*, 3412–3442. (b) Croteau, R. *Chem. Rev.* **1987**, *87*, 929–954.

(4) (a) Yoder, R. A.; Johnston, J. N. *Chem. Rev.* **2005**, *105*, 4730–4756. (b) Wendt, K. U.; Schultz, G. E.; Corey, E. J.; Liu, D. R. *Angew. Chem., Int. Ed.* **2000**, *39*, 2812–2833. (c) Sutherland, J. K. In *Comprehensive Organic Synthesis*; Trost, B. M., Ed.; Pergamon Press, 1991; Vol. 1, pp 341−377. (d) Bartlett, P. A. In *Asymmetric Synthesis*; Morrison, J. D., Ed.; Academic Press: New York, 1984; Vol. 3, pp 341−409.

(5) Trost, B. M.; Toste, F. D.; Pinkerton, A. B. *Chem. Rev.* **2001**, *101*, 2067–2096.

(6) (a) Chianese, A. R.; Lee, S. J.; Gagné, M. R. *Angew. Chem., Int. Ed.* **2007**, *46*, 4042–4059, and references therein. (b) Fürstner, A.; Davies, P. W. *Angew. Chem., Int. Ed.* **2007**, *46*, 3410–3449. (c) Liu, C.; Bender, C. F.; Han, X.; Widenhoefer, R. A. *Chem. Commun.* **2007**, 3607–3618. (d) Zhang, L.; Sun, J.; Kozmin, S. A. *Adv. Synth. Catal.* **2006**, *348*, 2271–2296. (e) Ma, S.; Yu, S.; Gu, Z. *Angew. Chem., Int. Ed.* **2006**, *45*, 200–203. (f) Méndez, M.; Mamane, V.; Fürstner, A. *Chemtracts: Org. Chem.* **2003**, *16*, 397–425.

(7) For several lead references, see refs 6b, 6d, and: (a) Hashmi, A. S. K *Chem. Rev* **2007**, *107*, 3180–3211. (b) Hashmi, A. S. K.; Hutchings, G. J. *Angew. Chem., Int. Ed.* **2006**, *45*, 7896–7936. (c) Widenhoefer, R. A.; Han, X. *Eur. J. Org. Chem.* **2006**, *455*, 5–4563.

(8) For a review on the stereoselective synthesis of cyclopropanes, see: (a) Lebel, H.; Marcoux, J.-F.; Molinaro, C.; Charette, A. B. *Chem. Rev* **2003**, *103*, 977–1050. For reviews focusing on electrophilic methods, see: (b) Bruneau, C. *Angew. Chem., Int. Ed.* **2005**, *44*, 2328–2334. (c) Taylor, R. E.; Engelhardt, F. C.; Schmitt, M. J. *Tetrahedron* **2003**, *59*, 5623–5634.

10.1021/om800760x CCC: $40.75
Publication on Web 03/16/2009

Scheme 1

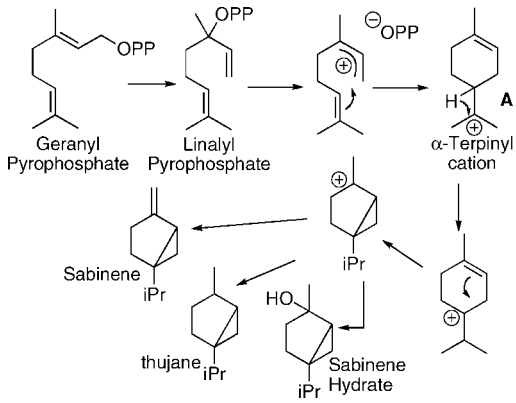

Scheme 2

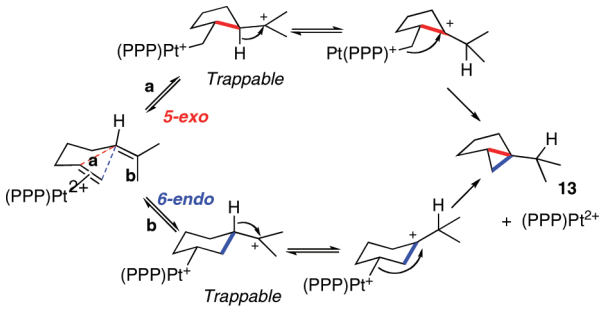

which after a 1,2-hydride shift and a second cation-olefin cyclization (transannular this time) provides the skeleton of the thujanes. A regiochemically parallel sequence of steps for the cycloisomerization of β-citronellene to *cis*-thujane was proposed for the Pt-catalyzed reaction (i.e., initial cyclohexyl ring formation followed by 1,2-hydride shift and transannular ring formation, Scheme 2).[12,13] Also consistent with the data was a separate sequence of steps wherein the first C−C bond forming reaction generated the five-membered ring, which after a 1,2-hydride shift and cyclopropanation provided the bicyclopropane product.[9,10] Since cationic intermediates corresponding to both an initiating 6-endo and 5-exo ring forming reaction could be trapped, it was not possible to differentiate between these two possible pathways. Since C−C bond formation had been shown to be rapid and reversible and 1,2-hydride shifts are typically fast, we postulated that the two pathways would ultimately be distinguished by the competitive rates of their cyclopropanation steps.

Although little is know about the details of the Pt-mediated cyclopropanation steps, the addition of a metal−carbon bond to a fully formed or incipient γ-carbocation has been previously studied for M = Ti,[14] Fe,[15] and Sn.[16] In all three cases, the reactions are known to be stereospecific and double invertive at each center (e.g., eq 3),[13] consistent with a reaction proceeding via a W conformation (in red) that orients the two leaving groups.

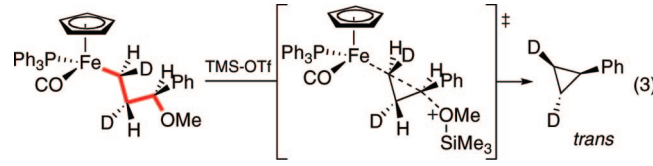

In the present case, one could a priori see how the annulative reaction pathway (5-exo) could easily accommodate the W conformer (Scheme 2); however, the conformation penalties and/or benefits imposed by confining the cation and the metal into a cyclohexane ring (6-endo) were less obvious.

Computational methods have recently been used successfully to study related reactions such as Pd-promoted sigmatropic shifts[17] and Pd-catalyzed allylic rearrangements.[18] To gain insight into the sequence of steps describing the two pathways and additionally provide the first computational evaluation of the double invertive cyclopropanation reaction, we initiated a DFT study on the comparative reaction surfaces. The model complex chosen for evaluation utilized the triphos ligand stripped of its phenyl substituents.[19]

Computational Methods

Calculations have been performed using GAUSSIAN 03.[20] Ground state structures were optimized in the gas phase using the RB3LYP hybrid functional[21,22] in combination with the 6-31+G** basis set. Pt was modeled using the SDDALL basis set, which includes effective core potentials.[23] This combination of functional and basis set has been shown to give good agreement with both structure and vibrational frequencies for Pd and Pt complexes.[24] Transition states were located using QST2, QST3, or TS methods.[25] Frequency calculations were carried out in the gas phase to confirm the presence of transition states and minima, as well as to establish free energy, enthalpy, and entropy values. Except for structure **9**, which was found to feature one negligible imaginary frequency at 5.15i cm^{-1}, all structures are confirmed minima or transition states, respectively. Transition states connecting **6** and **12** and those between **6** and **13** were confirmed by IRC calculations. In the case of the other transition states the motion associated with the imaginary frequencies supported their nature.

Molecular orbitals were visualized using Molekel.[26]

Results and Discussion

Intermediates and transition states were identified for both the 5-exo and the 6-endo pathways resulting in the formation

(9) (a) Feducia, J.; Campbell, A. N.; Doherty, M. Q. *J. Am. Chem. Soc.* **2006**, *128*, 13290–13297. (b) Kerber, W. D.; Gagné, M. R. *Org. Lett.* **2005**, *7*, 3379–3381. (c) Kerber, W. D.; Koh, J. H.; Gagné, M. R. *Org. Lett.* **2004**, *6*, 3013–3015.

(10) For an insightful study of the competition between cyclopropanation and alternative cycloisomerization processes in intermolecular olefin coupling with PNP-pincer ligated Pd and Pt catalysts, see: Cucciolito, M. E.; D'Amora, A.; Vitagliano, A. *Organometallics* **2005**, *24*, 3359–3361.

(11) Croteau, R. In *Recent Developments in Flavor and Fragrance Chemistry: Proceedings of the 3rd International Harmann & Reimer Symposium*; VCH: Weinheim: 1993; pp 263−273.

(12) For early studies documenting the generation of carbenium ions from alkenes and alkynes by Pt complexes, see: Chisolm, M. H.; Clark, H. C. *Acc. Chem. Res.* **1973**, *6*, 202–209.

(13) For additional examples of our work on the generation of carbocations from alkenes and Pd(II) and Pt(II), see: (a) Koh, J. H.; Gagné, M. R. *Angew. Chem., Int. Ed.* **2004**, *43*, 3459–3461. (b) Koh, J. H.; Mascarenhas, C.; Gagné, M. R. *Tetrahedron* **2004**, *60*, 7405–7410. (c) Korotchenko, V. N.; Gagné, M. R. *J. Org. Chem.* **2007**, *72*, 4877–4881. (d) Mullen, C. A.; Gagné, M. R. *J. Am. Chem. Soc.* **2007**, *129*, 11880–11881. (e) Mullen, C. A.; Campbell, A. N.; Gagné, M. R. *Angew. Chem., Int. Ed.* **2008**, *47*, 6011–6014.

(14) Casey, C. P.; Strotman, N. A. *J. Am. Chem. Soc.* **2004**, *126*, 1699–1704.

(15) (a) Casey, C. P.; Smith, L. J. *Organometallics* **1989**, *8*, 2288–2290. (b) Brookhart, M.; Liu, Y. *J. Am. Chem. Soc.* **1991**, *113*, 939–944. (c) Brookhart, M.; Liu, Y.; Goldman, E. W.; Timmers, D. A.; Williams, G. D. *J. Am. Chem. Soc.* **1991**, *113*, 927–939.

(16) (a) Fleming, I.; Urch, C. J. *Tetrahedron Lett.* **1983**, *24*, 4591–4594. (b) McWilliam, D. C.; Balasubramanian, T. R.; Kuivila, H. G. *J. Am. Chem. Soc.* **1978**, *100*, 6407–6413.

(17) Siebert, M. R.; Tantillo, D. J. *J. Am. Chem. Soc.* **2007**, *129*, 868.

(18) Watson, M. P.; Overman, L. E.; Bergman, R. G. *J. Am. Chem. Soc.* **2007**, *129*, 5031.

Scheme 3. Intermediates Observed and Studied for the Conversion of Diene to 13[a]

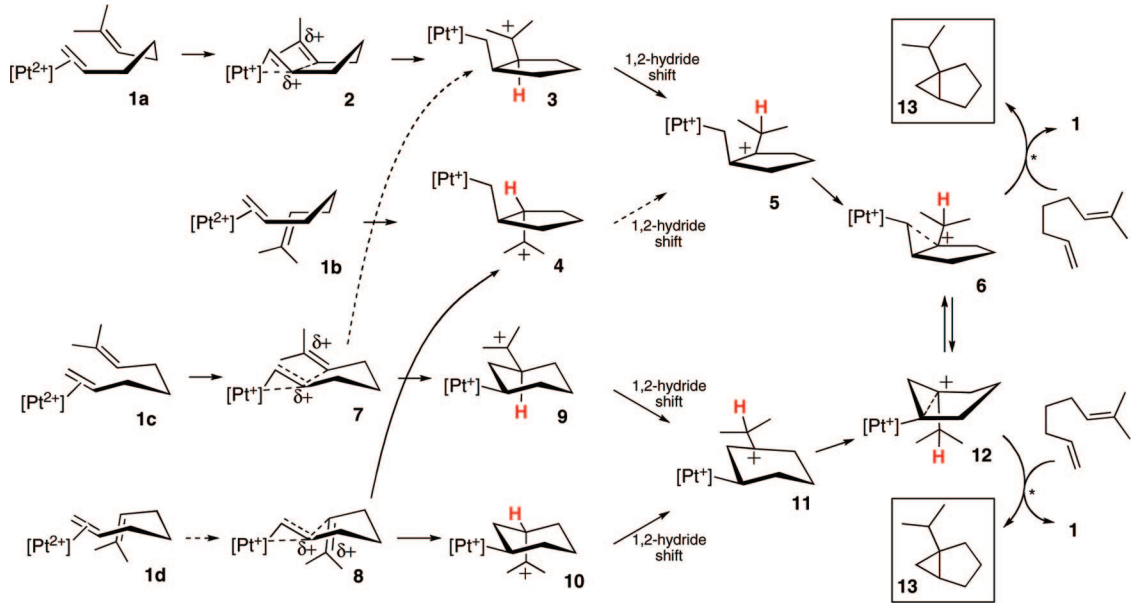

[a] Dashed arrows indicate no TS found. *Both associative and dissociative TSs calculated for **6** and **12**.

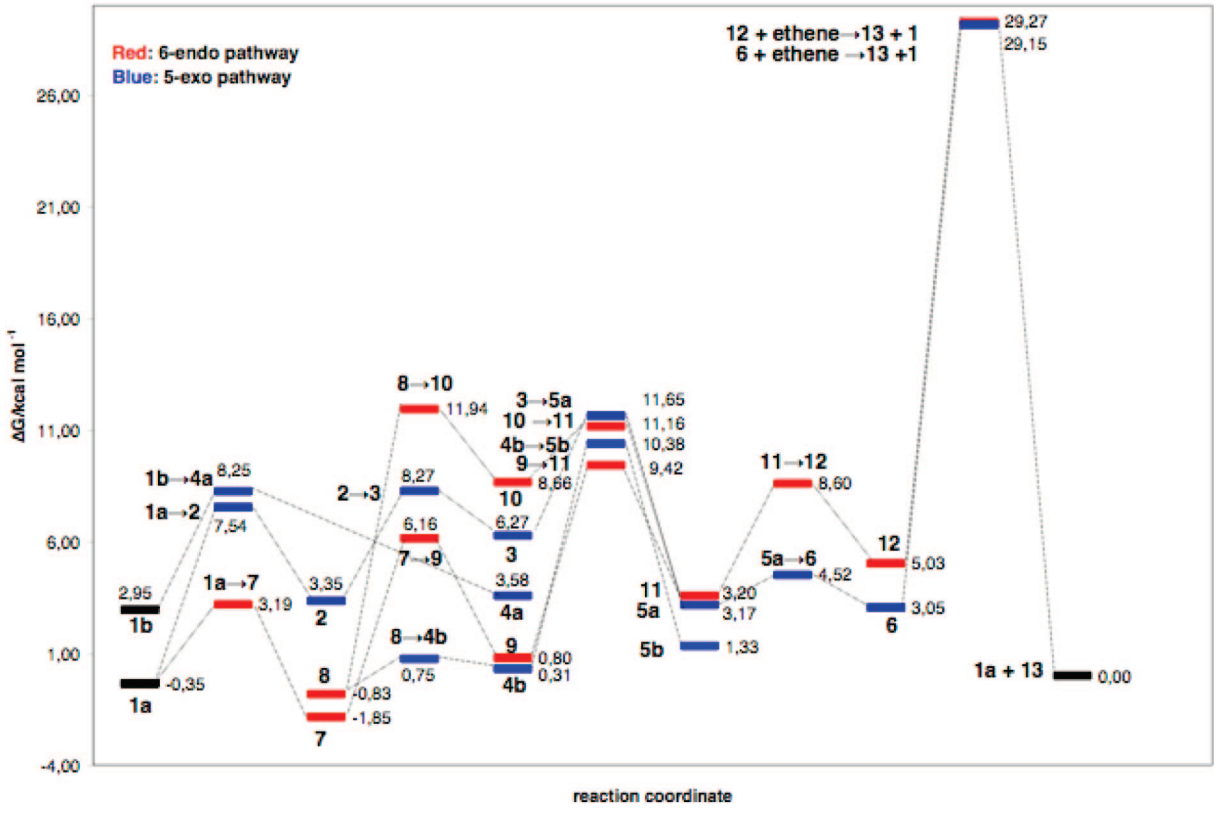

Figure 1. Energy pathway for the Pt-catalyzed cyclopropanation reaction; red for the 6-endo pathway and blue for the 5-exo pathway. Transition states of a particular reaction are indicated by the corresponding reactant and product number, connected by an arrow. The energy zero is taken as that of **1a** + the bicyclic product.

of the bicyclic product **13** (Scheme 2). Scheme 3 depicts all intermediates found for the 5-exo and 6-endo pathways. In some cases conformers of the intermediates were found, and they are distinguished by the alphabetical labels. For clarity not all conformers are indicated in Scheme 3, only some of those pertaining to **1**, where the diene is coordinated to the catalyst. In both pathways, depending on the initial conformation of the coordinated diene, multiple routes to the γ-carbocation were found. The energy profiles of the intermediates and the transition states connecting them are given in Figure 1; in this case the most significant conformers are included. The atom labelings for both pathways are shown in Figure 2.

Cyclization Regiochemistry: Nonclassical Alkene−Cation Interactions in "Slipped" η^2-Alkene Complexes. Although extended conformers were "normal" with regard to their Pt-η^2-alkene bonding, more curled conformers minimized to unusual

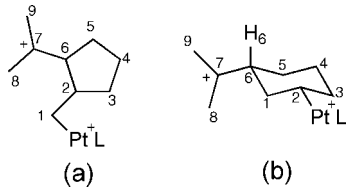

Figure 2. Labeling of atoms used in the (a) 6-endo and (b) 5-exo pathway.

structures wherein the Pt had slipped toward the terminus (C1) and generated positive character at C2,[27,28] which was further stabilized by the pendant alkene.[29] This latter interaction spread the charge over several centers (including C7)[30] and significantly distorted the Pt−C and C−C bonds. In three of the four cyclization conformers (**1a**, **1c**, and **1d**), this arrangement led to alkene slipped minima (**2**, **7**, and **8**) (Scheme 4).

Scheme 4. Conformer-Dependent Cyclization Profiles[a]

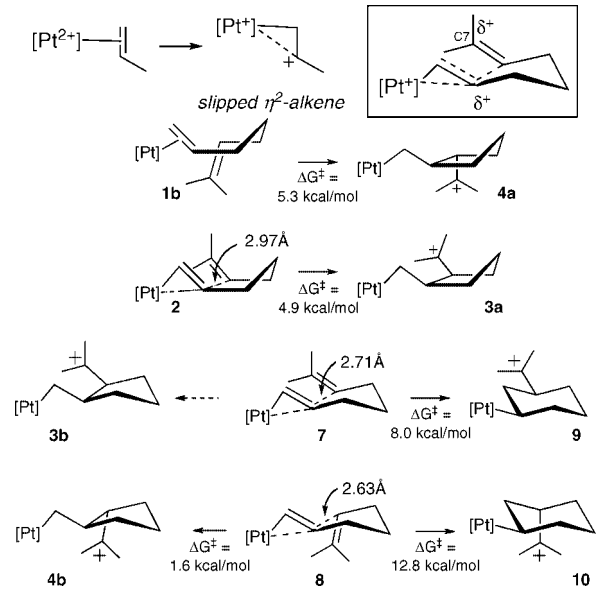

[a] The activation energies given are for gas phase calculations. Formal charges on the Pt moiety are not assigned.

The boat-like precyclization conformers (**1a**, **1b**, Scheme 3) smoothly traversed into the 5-exo reaction surface. Intermediate **2** completes the cyclization by fully adding the alkene to generate **3**, which has a *cis* arrangement of substituents on the cyclopentane ring (Scheme 4). The orientation positioning the two alkenes in a gauche relationship, **1b**, does not minimize to a nonclassical structure but instead completes the cyclization to **4** with a *trans* arrangement of groups. We speculate that these boat-like structures do not follow the 6-endo mode since this pathway would form boat products.[31,32]

When the precyclization conformers are chairlike (**1c** and **1d**, Scheme 3), these lead to similarly chairlike nonclassical alkene structures (**7** and **8**, Scheme 4). Compound **8** efficiently completes a 5-exo cyclization with a low activation barrier to a conformer of **4** (∼1.6 kcal/mol), but it is also able to execute a higher energy 6-endo cyclization to form **10** (∼12.8 kcal/mol). Noteworthy in the conversion of **8** to **10** is the motion that couples the 1,2-shift of the Pt from the terminal carbon to the internal carbon and the reciprocating 2,1-shift of the stabilizing alkene from the internal to the terminal position. This provides a mechanism for migrating the alkene to the terminus while minimizing positive charge buildup on the least substituted carbon center.

Once these intermediate conformers were reached, we assume rapid interconversion via low-energy processes (ring flips, etc.). The barriers for these cyclizations are considerably below the later ones, indicating that the competing pathways are not being differentiated in the first C−C bond-forming cyclization.

1,2-Hydride Shifts. The next step in both pathways is a 1,2-hydride shift that moves the positive charge from a carbon outside the ring to a ring-contained one, forming **5** and **11**. The barriers calculated for this process are low, ranging from 2.5 to 10.1 kcal mol^{-1}. Yet again the differences between the 5-exo and 6-endo pathways are insufficient to differentiate the two

(19) For recent and/or relevant works that computationally examine processes of relevance to terpene biosynthesis see: (a) Gutta, P.; Tantillo, D. J. *J. Am. Chem. Soc.* **2006**, *128*, 6172–6179. (b) Rajamani, R.; Gao, J. *J. Am. Chem. Soc.* **2003**, *125*, 12768–12781. (c) Nishizawa, M.; Yadav, A.; Imagawa, H.; Sugihara, T. *Tetrahedron Lett.* **2003**, *44*, 3867–3870. (d) Jenson, C.; Jorgensen, W. L. *J. Am. Chem. Soc.* **1997**, *119*, 10846–10854. (e) Gutta, P.; Tantillo, D. *J. Org. Lett.* **2007**, *9*, 1069. (f) Hong, Y. J.; Tantillo, D. J. *Org. Lett.* **2006**, *8*, 4601. (g) Matsuda, S. P. T.; Wilson, W. K.; Xiong, Q. *Org. Biomol. Chem.* **2006**, *4*, 530.

(20) Frisch, M. J.; Trucks, G. W.; Schlegel, H. B.; Scuseria, G. E.; Robb, M. A.; Cheeseman, J. R.; Montgomery, J. A., Jr.; Vreven, T.; Kudin, K. N.; Burant, J. C.; Millam, J. M.; Iyengar, S. S.; Tomasi, J.; Barone, V.; Mennucci, B.; Cossi, M.; Scalmani, G.; Rega, N.; Petersson, G. A.; Nakatsuji, H.; Hada, M.; Ehara, M.; Toyota, K.; Fukuda, R.; Hasegawa, J.; Ishida, M.; Nakajima, T.; Honda, Y.; Kitao, O.; Nakai, H.; Klene, M.; Li, X.; Knox, J. E.; Hratchian, H. P.; Cross, J. B.; Bakken, V.; Adamo, C.; Jaramillo, J.; Gomperts, R.; Stratmann, R. E.; Yazyev, O.; Austin, A. J.; Cammi, R.; Pomelli, C.; Ochterski, J. W.; Ayala, P. Y.; Morokuma, K.; Voth, G. A.; Salvador, P.; Dannenberg, J. J.; Zakrzewski, V. G.; Dapprich, S.; Daniels, A. D.; Strain, M. C.; Farkas, O.; Malick, D. K.; Rabuck, A. D.; Raghavachari, K.; Foresman, J. B.; Ortiz, J. V.; Cui, Q.; Baboul, A. G.; Clifford, S.; Cioslowski, J.; Stefanov, B. B.; Liu, G.; Liashenko, A.; Piskorz, P.; Komaromi, I.; Martin, R. L.; Fox, D. J.; Keith, T.; Al-Laham, M. A.; Peng, C. Y.; Nanayakkara, A.; Challacombe, M.; Gill, P. M. W.; Johnson, B.; Chen, W.; Wong, M. W.; Gonzalez, C.; Pople, J. A. *Gaussian 03, Revision C.02*; Gaussian, Inc.: Wallingford, CT, 2004.

(21) Lee, C.; Yang, W.; Parr, R. *Phys. Rev.* **1998**, *B37*, 785–789.

(22) Becke, A. *J. Chem. Phys.* **1993**, *98*, 5648.

(23) (a) Fuentealba, P.; Preuss, H.; Stoll, H.; Szentpaly, L. v. *Chem. Phys. Lett.* **1989**, *89*, 418. (b) Szentpaly, L. v.; Fuentealba, P.; Preuss, H.; Stoll, H. *Chem. Phys. Lett.* **1982**, *93*, 555. (c) Fuentealba, P.; Stoll, H.; Szentpaly, L. v.; Schwerdtfeger, P.; Preuss, H. *J. Phys. B* **1983**, *16*, 1323. (d) Stoll, H.; Fuentealba, P.; Schwerdtfeger, P.; Flad, J.; Szentpaly, L. v.; Preuss, H. *J. Chem. Phys.* **1984**, *81*, 2732. (e) Fuentealba, P.; Szentpaly, L. v.; Preuss, H.; Stoll, H. *J. Phys. B* **1985**, *18*, 1287.

(24) (a) Nakamura, I.; Bajracharya, G. B.; Wu, H.; Oishi, K.; Mizushima, Y.; Gridnev, I. D.; Yamamoto, Y. *J. Am. Chem. Soc.* **2004**, *126*, 15423–15430. (b) Yang, G.; Jin, C.; Hong, J.; Guo, Z.; Zhu, L. *Spectrochim. Acta A* **2004**, *60*, 3187–3195.

(25) (a) Peng, C.; Schlegel, H. B. *Isr. J. Chem.* **1993**, *33*, 449. (b) Peng, C.; Ayala, P. Y.; Schlegel, H. B.; Frisch, M. J. *J. Comput. Chem.* **1996**, *17*, 49.

(26) Gonzalez, C.; Schlegel, H. B. *J. Chem. Phys.* **1990**, *94*, 5523–5527.

(27) (a) Eisenstein, O.; Hoffmann, R. *J. Am. Chem. Soc.* **1981**, *103*, 4308–4320, See also. (b) Senn, H. M.; Blöchl, P. E.; Togni, A. *J. Am. Chem. Soc.* **2000**, *122*, 4098–4107.

(28) Vitagliano and co-workers have proposed such a slipping as the first step of an electrophilic alkene activation by Pd and Pt complexes on several occasions; see for example: (a) Hahn, C. *Chem.−Eur. J.* **2004**, *10*, 5888–5899. (b) Hahn, C.; Cucciolito, M. E.; Vitagliano, A. *J. Am. Chem. Soc.* **2002**, *124*, 9038–9039. (c) Hahn, C.; Vitagliano, A.; Giordano, F.; Taube, R. *Organometallics* **1998**, *17*, 2060–2066. (d) Goldschmidt, Z.; Gottlier, H. E.; Cohen, D. *J. Organomet. Chem.* **1985**, *294*, 219–233. See also ref 27.

(29) (a) For a computational study wherein the cyclogenerated carbenium ion was trapped by an alcohol in a bicyclization reaction by a (PPP)Pt-dication, see: (b) Nowroozi-Isfahani, T.; Musaev, D. G.; Morokuma, K.; Gagné, M. R. *Organometallics* **2007**, *26*, 2540–2549.

(30) For a classic treatise on nonclassical carbocations, see: (a) Winstein, S. *Q. Rev. (London)* **1969**, *23*, 1411. (b) Bartlett, P. D. *Nonclassical Ions*; W. A. Benjamin Inc: New York, 1965. (c) Brown, H. C. *The Nonclassical Ion Problem*; Plenum Press: New York, 1977. (d) For a more recent perspective, see: Olah, G. A. *J. Org. Chem.* **2001**, *66*, 5943–5957.

(31) This possibility was not computationally investigated.

(32) For important computational studies of the cascade cation-olefin process involved in sterol biosynthesis, see ref 19d.

Table 1. Geometrical Parameters of 6, 12, and 13 (product)

bond length/Å	6	12	13
Pt1−C1	2.18	2.18	
C1−C6	2.28	2.24	1.52
C1−C2	1.58	1.60	1.51
C2−C6	1.47	1.46	1.52
bond angle/deg	**6**	**12**	**13**
Pt1−C1−C2	115.93	109.95	
C1−C2−C6	96.65	94.16	60.13
C2−C6−C1	43.62	45.36	59.91

Table 2. Bond Lengths and Angles in the TS Connecting 6 and 12

bond length/Å	6 → 12	6 → 12 (+ethene)
Pt1−C1	2.52	4.42
Pt1−C2	2.59	4.77
C1−C6	1.55	1.52
C1−C2	1.65	1.52
C2−C6	1.48	1.51
Pt1−ethene		2.37
bond angle/deg	**6 → 12**	**6 → 12 (+ethene)**
Pt1−C1−C2	73.47	93.89
C1−C2−C6	59.11	60.10
C2−C6−C1	65.70	60.27

pathways. The tertiary carbocations **5** and **11** are estimated to be very close in energy, and it may be assumed that both are accessed in the course of the reaction.

Nonclassical Carbocations[12,30] The carbocations **5** and **11** have bond angles and lengths associated with classical carbocations. In the course of seeking routes to cyclopropanation two further readily accessible intermediates, **6** and **12**, were discovered. Key dimensions are given in Table 1. The conformation of these intermediates is discussed further below, but it is apparent from, for example, the closing of the C1−C2−C6 angle that they may well lie on the pathway to formation of the three-membered cyclopropane ring. Activation barriers to their formation lie in the range 1.4 to 5.5 kcal mol^{-1}.

Given the similarity of their structures, it came as no surprise that in searching for the ring closure pathway, two transition states were identified connecting **6** to **12**. One involved no additional species, whereas the other had a molecule of ethene associated with the Pt (introduced to simulate an associative pathway for cyclopropanation). Corresponding geometric parameters can be found in Table 2. Comparison of the free energies of the two possible transition states (Figure 3) revealed that the values are extremely similar.

Cyclopropanation. In the final step of the reaction, in both routes, the organic moiety is lost from the Pt catalyst to form

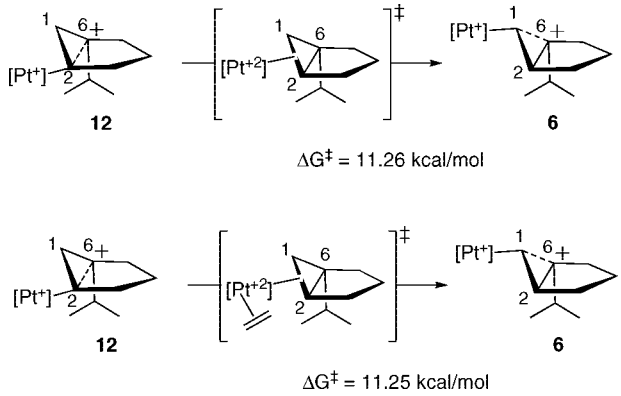

Figure 3. Energy diagram illustrating the interconversion of **12** and **6**, both with and without the benefit of ethylene.

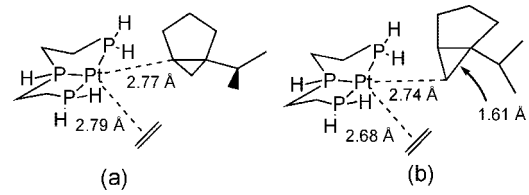

Figure 4. Proposed associative cyclopropanation transition states involving ethene (a) 6-endo and (b) 5-exo.

Table 3. Geometrical Parameters for Cyclopropanation Transition States Involving Ethene

	13 (product)	5-exo 6 → 13 + 1 TS	6-endo 12 → 13 + 1 TS
C1−C2/Å	1.52	1.55	1.52
C2−C6/Å	1.52	1.48	1.50
C1−C6/Å	1.52	1.61	1.57
Pt1−C2/3/Å		2.74	2.76

the cyclopropane ring. Both dissociative and associative mechanisms were considered. In modeling the associative transition state a molecule of ethene was used as the displacing ligand instead of the diene starting material for computational expediency.

In the case of the 6-endo pathway, the breaking Pt−C bond in the transition state was slightly shorter than the distance between the metal center and the incoming alkene (Figure 4). The opposite, however, was found for the 5-exo pathway. Also, in the case of the 6-endo pathway the distances between the metal center and the incoming/leaving groups were generally longer than for the 5-exo pathway. However, the cyclopropanation was more advanced for the 6-endo pathway, as evidenced by that transition state showing the shorter C1−C6 distance (Table 3). Furthermore, the ethene C−C bond lengths in the transition states are 1.35 Å (6-endo) and 1.35 Å (5-exo), confirming an interaction between the metal center and the alkene.

Consideration of the corresponding activation barriers for the cyclopropanation step (Figure 5) reveals that cyclopropanation

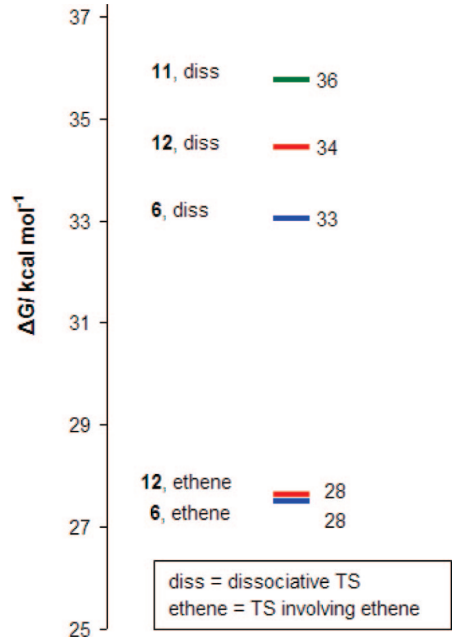

Figure 5. Energies of dissociative and associative cyclopropanation transition states.

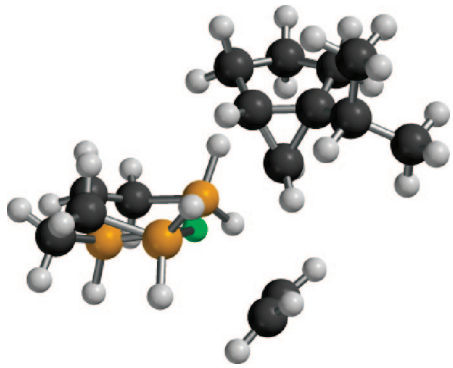

Figure 6. Associative TS for the conversion of **6** to **13** and the ethylene adduct of the catalyst.

is the rate-determining step for both pathways.[33] The presence of ethene reduces the free energy of the cyclopropanation transition state in the gas phase. The structure of the associative cyclopropanation transition state (from **6**) is shown in Figure 6 and has the trigonal-bipyramidal conformation generally assumed for substitution of Pt(II) complexes.[34]

The similarity of the two competing associative transition state energies does not allow the two pathways to be energetically differentiated, though the preceding low-energy steps do have their own preferred pathways. Furthermore, comparison between the activation energies for the cyclopropanation step (ca. 28 kcal mol^{-1}) and the interconversion between **6** and **12** (ca. 11−13 kcal mol^{-1}, respectively) reveals that interconversion between **6** and **12** is far more likely than cyclopropanation. This, therefore, suggests that regardless of which regio-direction the first cyclization takes (6-endo vs 5-exo), a late stage pathway exists for interconverting the competing reaction surfaces. In that sense the two pathways are not actually competing, and the question of which mechanism to product becomes moot; both mechanisms lead to product via a common intermediate.

The above discussion of the 6-endo pathway versus 5-exo pathway should thus be supplanted and the question reformulated as to whether the annulative or transannular arrangement is more favorable for cyclopropanation. Since **12** is 2 kcal/mol higher than **6** and their $\Delta G^{\ddagger}$ are the same, this would point to a slight preference for the transannular situation. One could reasonably also conclude that they are nearly identical and neither is especially advantageous.

Overall $\Delta G^{\ddagger}$ between the lowest energy intermediate, **7**, and the cyclopropanation transition state is 31 kcal/mol, rather larger than suggested by the experimental conditions.[35,36] This breaks down to an activation enthalpy of 18 kcal/mol and an activation entropy of −47 cal/K/mol. The large negative $\Delta S^{\ddagger}$ is a consequence of the associative transition state. Gas phase calculations are not really appropriate for modeling reactions in solution, where there is a change in the number of moles between reactant and product, because they overestimate

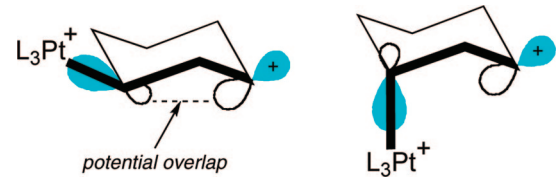

Figure 7. Schematic diagram depicting (a) a W-shaped and (b) a non-W-shaped structure. The p orbital of the cationic carbon forms a stroke of the W.

translational and rotational entropy.[37] On the other hand $\Delta H^{\ddagger}$, which does not include entropy effects, will underestimate $\Delta G^{\ddagger}$ for an associative reaction. The values of 18 and 31 may be regarded as lower and upper estimates for the free energy of activation for this reaction. Thus the proposed mechanism is compatible with the experimental reaction conditions.

Stereochemical Requirements: Importance of W-Shaped Structures in the Cyclopropanation Step. Cyclopropanation Step. The two intermediates **6** and **12** were found to play a decisive role in the cyclopropanation step of this reaction. Both feature a W conformation, which has been observed in numerous noncationic cyclopropanation reactions.[14] Key structural parameters for **6** and **12** are given in Table 1 together with those for the product **13**. Of particular note are the short C1−C6 distance and the small C1−C2−C6 angles of the carbocations, identifying **6** and **12** as nonclassical structures. In this particular case this arrangement allows overlap between the empty p orbital on the carbocation, which forms a stroke of the W, and the bonding Pt−C orbital (Figures 7 and 8). Furthermore, a W conformation features the least steric hindrance (Figure 7). Both of these factors should facilitate C−C bond formation. Indeed, visualization of the HOMO, as well as NBO analysis (Table 4) of intermediates **6** and **12**, confirms that cyclopropanation is considerably advanced in W structures compared to different conformers. Generally speaking, the Pt−C1 occupancy is smaller for W-shaped structures (mirrored by an increase in Pt−C1 bond length), whereas the p-orbital occupancy is greater than in non-W-shaped analogues. In addition the interaction energy for W structures arising from donation of electron density from the Pt−C orbital into the empty p orbital on C6 via the back lobe of the Pt−C1 bond, an interaction known as homohyperconjugation or percaudal ("through the tail") conjugation,[38] is considerably greater. This is reflected by the considerably shorter C1−C6 bond length in W conformers (up to 0.36 Å).

Protonated Analogues. The question that naturally arises is whether hyperconjugation is restricted to Pt (metal) systems or whether these may occur in any W conformation. In order to assess this, Pt(triphos) was replaced by H and the intermediates were reoptimized. Figure 9 shows the minimum energy struc-

(33) This is therefore an example of a Curtin−Hammett controlled process. See: Seeman, J. I. *Chem. Rev* **1983**, *83*, 84−134.

(34) Five-coordinate triphos-Pd complexes are known; see: López-Torres, M.; Fernández, A.; Fernández, J. J.; Suárez, A.; Pereira, M. T. M., O. J.; Vila, J. N.; Adams, H. *Inorg. Chem.* **2001**, *40*, 4583–4587.

(35) Based on a turnover frequency of ∼1 per hour, we calculate an activation energy of 23−24 kcal/mol for the catalytic reaction in nitromethane (40 °C); see ref 9b. The [(triphos)Pt][BF_4][NTf_2] catalyst was used at 5 mol % and was generated in situ from the protonolysis of [(triphos)Pt-CH_3][BF_4] with $HNTf_2$ (to release methane) in the presence of 1 equiv of acetone (to generate an acetone adduct). Addition of diene substrate to this catalyst displaced the acetone and generated an alkene adduct, which served as the catalyst resting state during catalysis.

(36) The disparity between the calculated (∼31 kcal mol^{-1}) and experimentally observed barrier (23−24 kcal mol^{-1}) was more than expected. We note that the cyclopropanation rates are especially sensitive to solvent polarity (CH_3NO_2 > CH_2Cl_2), suggesting that gas phase calculations will overestimate $\Delta G^{\ddagger}$.

(37) Green, J. C.; Herbert, B. J.; Lonsdale, R. *J. Organomet. Chem.* **2005**, *690*, 6054.

(38) Green, A. J.; White, J. M. *Aust. J. Chem.* **1998**, *51*, 555–563.

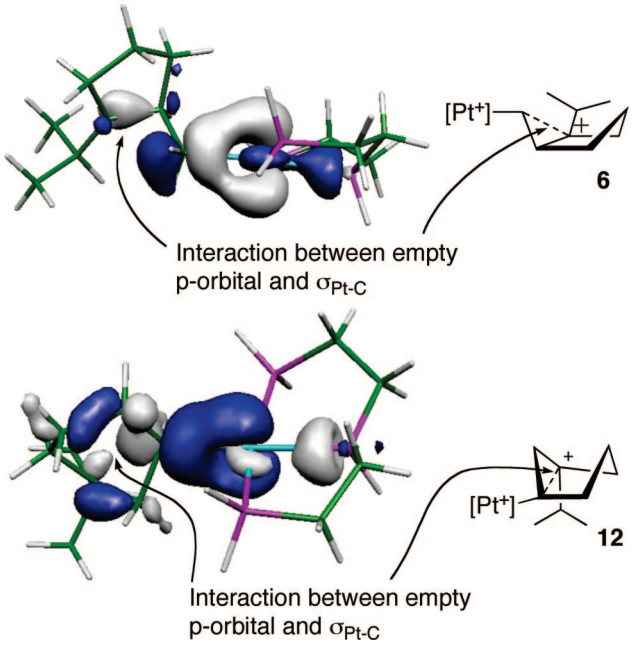

Figure 8. Orbitals involved in a percaudal interaction: (top) HOMO of **6**, (bottom) HOMO of **12**.

Table 4. Data Indicating Facilitated Cyclopropanation for W-Shaped Conformers

structure name	W shape?	Pt−C1/Å	Pt−C1 occupancy	p orbital occupancy	C1−C6/Å	*E*(int)[a] /kcal mol^{-1}
5	yes	2.17	1.83	0.47	2.29	1.60
6	yes	2.18	1.83	0.47	2.28	5.26
11	yes	2.17	1.84	0.49	2.34	3.34
12	yes	2.18	1.81	0.50	2.25	4.89
9b	no	2.15	1.91	0.45	2.50	0.57
5c	no	2.15	1.90	0.45	2.64	<0.50

[a] Interaction energy, *E*(int), between empty p orbital and bonding Pt−C1 orbital.

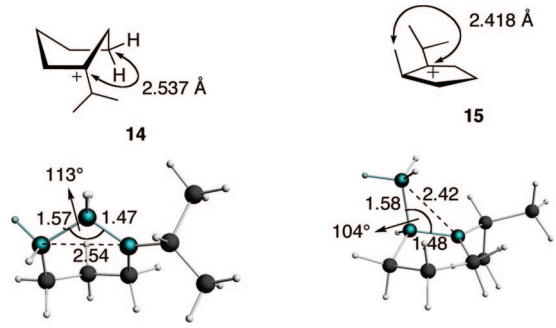

Figure 9. Schematic diagrams of **14** and **15** with key bond lengths (Å) and angles (deg).

tures, **14** and **15**, found for the 6-endo and 5-exo pathways, respectively. The conformations of **14** and **15** are, generally speaking, similar to the metal analogues, **12** and **6**. In a like manner to the Pt systems the protonated structures **14** and **15** adopt a W structure.

Table 5 compares structural parameters of the protonated intermediates with the Pt analogues. The C1−C6 distances and the C1−C2−C6 angles, as well as a corresponding NBO analysis, suggest that a percaudal interaction is present in protonated structures, but comparison of Pt and protonated systems (Table 5) reveals that hyperconjugation is less pronounced in the protonated analogues. The difference between C1−C6 distances in W and non-W shaped structures is 1.8 times

Table 5. Selected Bond Lengths and Angles in W and Non-W Structures of the 5-exo and 6-endo Pathways[a]

	protonated systems			Pt system		
	14	**15**	**16**	**12**	**6**	**5b**
W shape?	yes	yes	no	yes	yes	no
C1−C6/Å	2.54	2.42	2.62	2.25	2.28	2.64
C1−C2−C6/deg	113	104	121	94	96	122
C1−C3 or C4/Å	2.56	2.59	2.64	2.57	2.62	2.65

[a] Gas phase, rb3lyp/6-31+G**, **14** is the analogue of **12**, **15** is the analogue of **6**, and **16** is the analogue of **5b**.

Table 6. Most Important Geometric Parameters of 11 → 13 + 1, 12 → 13 + 1, and 13

bond lengths/Å	**11 → 13 + 1**	**12 → 13 + 1**	**13**
Pt1−C1	5.41	5.67	
C1−C6	1.61	1.58	1.52
C1−C2	1.50	1.50	1.52
C2−C6	1.51	1.51	1.52
bond angles/deg	**11 → 13 + 1**	**12 → 13 + 1**	**13**
C1−C2−C6	64.96	63.37	60.14
C2−C6−C1	57.25	57.94	59.91

larger in the Pt systems (ΔC1−C6(Pt) = 0.36 Å) compared to the protonated ones (ΔC1−C6(H) = 0.20 Å) (Table 3). This is reinforced by the corresponding interaction energies, namely, that between the Pt−C1 bonding orbital and the empty orbital on C6. Furthermore, non-W structures of Pt and nonmetal systems are extremely similar in terms of geometrical parameters, whereas these deviate substantially in the case of W systems. In particular, the C1−C6 distances of the W-shaped Pt systems are appreciably shorter (between 0.14 and 0.29 Å) than those of the protonated analogues. In the case of W structures, the C1−C2−C6 angle is appreciably smaller for the Pt system than the corresponding protonated analogue, indicating that the percaudal interaction is weaker in the protonated systems (ΔC1−C2−C6(5exo) = 7.9°, ΔC1−C2−C6(6endo) = 18.2°). This reflects the above-mentioned finding that the C1−C6 distances are shorter for the Pt analogues.

Last, but not least, it is noteworthy to mention that the only geometric parameters that change significantly on going from a non-W structure to a W structure are the C1−C6 bond length and the C1−C2−C6 bond angles (Table 3). This is a strong indication that homohyperconjugation and no other interaction is responsible for the facilitated C−C bond formation.

It is also possible that a percaudal interaction also plays a role in the 1,2-hydride shifts, either by destabilizing the ground state (donation of electron density from the bonding Pt−C2 into the antibonding C6−H orbital) or by stabilizing the transition state. No correlation could be found (neither in the starting material nor in the transition state) between a W conformation and the activation energies, geometric parameters, or orbital occupancies associated with the 1,2-hydride shift.

Direct Cyclopropanation Reactions. 6-endo Pathway. In light of the fact that a W structure is required for a facile cyclopropanation, one may question the need of intermediate **12**, since structure **11**, the preceding intermediate, actually features the required conformation. A cyclopropanation transition state that directly connected **11** with the desired products therefore would render the interconversion from **11** to **12**, which was associated with a 5.40 kcal mol^{-1} activation barrier, unnecessary.

A corresponding transition state, which features a W structure, was located for **11 → 13 + 1** with a structure similar to the ethene free structure, **12 → 13 + 1**. The most important geometric parameters are listed in Table 6 along with the

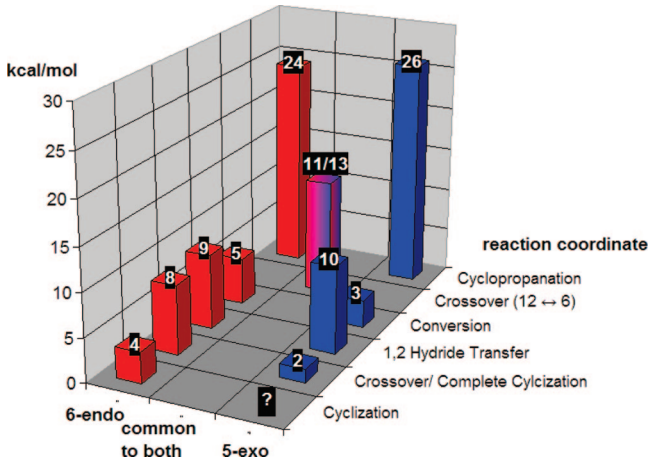

Figure 10. Activation energies for the two possible 5-exo and 6-endo pathways.

corresponding data from **10**. As can be seen from Table 6, the two transition states **11** → **13** + **1** and **12** → **13** + **1** have very similar geometric parameters. However, closer analysis of the data suggests that **10** cyclopropanates more readily than **11** (shorter C1−C6 bond length, smaller Pt−C occupancy, longer Pt−C bond length, etc., in the case of **12** → **13** + **1**). Indeed, the free energy, ΔG_{298}, of the reaction **11** → **13** + **1** is 1.31 kcal mol^{-1} higher than the route **12** → **13** + **1**. Hence, as the cyclopropanation reaction was found to be the rate-determining step, the pathway involving the unconventional intermediate **12** is more likely to occur.

5-exo Pathway. Similar to the 6-endo case, direct cyclopropanation from the W structure **5** may occur, avoiding **6**. However, the activation barrier for conversion of **5** into **6** is only 1.43 kcal mol^{-1}, and the geometric features of the two intermediates are nearly identical. Thus, no appreciable advantage of direct cyclopropanation from **5** is expected.

Conclusions

The computational studies provide strong supporting evidence that the cyclopropanation step is rate determining in the production of **13**, as has been proposed. However, contrary to what was expected, the cyclopropanation transition states for the 5-exo and 6-endo pathways have very similar free energy values ($\Delta G_{298} = 0.12$ kcal mol^{-1}). In addition, the difference in the free energies of activation, $\Delta G^{\ddagger}_{298}$, between the 5-exo and 6-endo pathway for the cyclopropanation step is only 1.86 kcal mol^{-1}. Figure 10 shows the energy surface for some of the key transformations, which gives an effective visualization of a slightly rumpled energy surface before the final transformation. It has also been demonstrated that interconversion between the two channels via **6** and **12** (and via **4b** and **10** through **8**) is more facile than cyclopropanation; thus all pathways to the two interconverting intermediates are possible and all intermediates are likely to be sampled.

A W conformation is vital for cyclopropanation, but does not play a decisive role in the case of the 1,2-hydride shift. Percaudal interactions are not restricted to Pt (or other metals, as were reported in the literature), but are present also in protonated systems but to a significantly lesser extent. It is therefore likely that homohyperconjugation occurs in every W system, but the degree to which it facilitates ring closure will vary. In the reaction examined here, there appears to be little to discriminate between annulative or transannular cyclopropanation.

Acknowledgment. M.R.G. wishes to thank the National Institutes of General Medicine for generous support (GM-60578). J.C.G. and F.B. thank St. Hugh's College, Oxford, for support.

Supporting Information Available: Cartesian coordinates for intermediates and transition states. Ball and stick diagrams of optimized structures. Imaginary frequencies. Zero-point energy corrections, entropy corrections (298 K), ΔE(SCF), ΔH(298 K), and ΔG(298 K). This material is available free of charge via the Internet at http://pubs.acs.org.

OM800760X